The distribution of the ring current: Cluster observations

Ann. Geophys., 29, 1655–1662, 2011
www.ann-geophys.net/29/1655/2011/
doi:10.5194/angeo-29-1655-2011

Annales Geophysicae

The distribution of the ring current: Cluster observations

Q.-H. Zhang[1], M. W. Dunlop[2], M. Lockwood[2], R. Holme[3], Y. Kamide[1], W. Baumjohann[4], R.-Y. Liu[1], H.-G. Yang[1], E. E. Woodfield[5], H.-Q. Hu[1], B.-C. Zhang[1], and S.-L. Liu[1]

[1]SOA Key Laboratory for Polar Science, Polar Research Institute of China, Shanghai, China
[2]SSTD, Rutherford Appleton Laboratory, Chilton, Didcot, Oxfordshire, UK
[3]Department of Earth and Ocean Sciences, University of Liverpool, Liverpool, UK
[4]Space Research Institute, Austrian Academy of Sciences, Graz, Austria
[5]Department of Communications Systems, University of Lancaster, Lancaster, UK

Received: 18 October 2010 – Revised: 13 September 2011 – Accepted: 15 September 2011 – Published: 28 September 2011

Abstract. Extending previous studies, a full-circle investigation of the ring current has been made using Cluster 4-spacecraft observations near perigee, at times when the Cluster array had relatively small separations and nearly regular tetrahedral configurations, and when the Dst index was greater than −30 nT (non-storm conditions). These observations result in direct estimations of the near equatorial current density at all magnetic local times (MLT) for the first time and with sufficient accuracy, for the following observations. The results confirm that the ring current flows westward and show that the in situ average measured current density (sampled in the radial range accessed by Cluster ∼4–4.5 R_E) is asymmetric in MLT, ranging from 9 to 27 nA m^{-2}. The direction of current is shown to be very well ordered for the whole range of MLT. Both of these results are in line with previous studies on partial ring extent. The magnitude of the current density, however, reveals a distinct asymmetry: growing from 10 to 27 nA m^{-2} as azimuth reduces from about 12:00 MLT to 03:00 and falling from 20 to 10 nA m^{-2} less steadily as azimuth reduces from 24:00 to 12:00 MLT. This result has not been reported before and we suggest it could reflect a number of effects. Firstly, we argue it is consistent with the operation of region-2 field aligned-currents (FACs), which are expected to flow upward into the ring current around 09:00 MLT and downward out of the ring current around 14:00 MLT. Secondly, we note that it is also consistent with a possible asymmetry in the radial distribution profile of current density (resulting in higher peak at ∼4–4.5 R_E). We note that part of the enhanced current could reflect an increase in the mean AE activity (during the periods in which Cluster samples those MLT).

Keywords. Magnetospheric physics (Current systems; Magnetospheric configuration and dynamics)

Correspondence to: Q.-H. Zhang
(zhangqinghe@pric.gov.cn)

1 Introduction

The existence of the westward equatorial ring current around the Earth at geocentric distances of about 2–9 R_E (R_E is a mean Earth radius) was first suggested by Singer (1957). It is understood in terms of the gradient and curvature drifts of energetic particles (∼1 keV to a few hundreds of keV), trapped in the geomagnetic field. Le et al. (2004) examined the 20 years of magnetospheric magnetic field data from the ISEE, AMPTE/CCE, and Polar missions, and showed that there are two ring currents: an inner one flowing eastward at ∼3 R_E, and the main westward ring current at ∼4–7 R_E for all levels of geomagnetic disturbances. The ring current evolution is dependent on particle injections during geomagnetic activity and on loss mechanisms (Daglis et al., 1999). Because simultaneous magnetic field measurements at multiple, geometrically favorable positions were unavailable prior to Cluster, it had been impossible to obtain a precise idea about the current response to magnetospheric changes. Cluster (Escoubet et al., 2001) has provided us with a unique opportunity to directly survey the distribution of the ring current.

The Cluster mission is composed of an array of four spacecraft carrying identical payloads. The spacecraft were launched in pairs in July and August 2000 into similar elliptical, polar orbits, each with a perigee of ∼4 R_E, an apogee of ∼19.6 R_E, and identical orbital periods of 57 h. A typical orbital orientation with respect to the model field lines is shown in Fig. 1. Due to the Earth's orbital motion, Cluster's orbits precess in the solar-magnetospheric (SM) coordinate system, so that every year all magnetic local times (MLT) are covered. For the Cluster perigee crossings, 00:00, 06:00, 12:00, and 18:00 MLT are sampled, respectively, in February, May, August, and November (Escoubet et al., 2001). The spacecraft formed a tetrahedral configuration that evolved around each orbit. The orbits were adjusted approximately once every 6–12 months via a sequence of maneuvers to vary the spatial scales between 100 km and a few R_E over the mission

Published by Copernicus Publications on behalf of the European Geosciences Union.

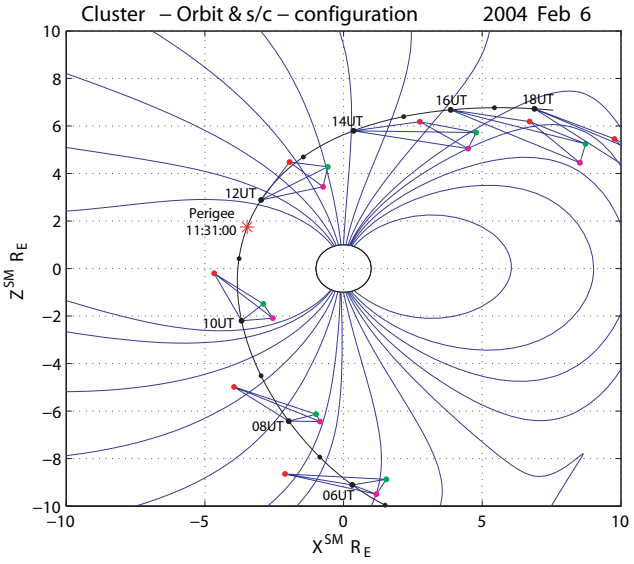

Fig. 1. Orbit plot in XZ plane in SM coordinates for night-side orientation orbit 555/556 on 6 February 2004. The orbit also shows the configuration of the Cluster spacecraft array as a tetrahedron (size scaled up by a factor of 80). Model geomagnetic field lines are drawn from the T96 model with the average inputting parameters: $P_{\rm dyn} = 1.76$ nPa, IMF $B_{\rm Y} = -3.89$ nT, IMF $B_{\rm Z} = -2.29$ nT, and Dst $= -18$ nT.

lifetime. For example, the four Cluster spacecraft had average separations of about 180 km during March/June 2002 and about 480 km between July 2003 and April 2004. Here, we have used 4-s data from one of the 11 experiments aboard each craft, the fluxgate-magnetometer (FGM) (Balogh et al., 2001). In-flight calibrations on FGM data routinely determine the maximum error in the data to within 0.1 nT.

The "Curlometer" technique has been developed to derive currents from four-point magnetic field measurements (Dunlop et al., 1988, 2002; Robert et al., 1998) based on Maxwell-Ampere's law

$$\mu_0 \boldsymbol{J} = \nabla \times \boldsymbol{B} - \varepsilon_0 \mu_0 \frac{\partial \boldsymbol{E}}{\partial t}$$

where the second term on the right-hand side is negligible for a highly conducting plasma, and the measurement of $\nabla \times \boldsymbol{B}$ assumes stationarity in the region of interest (i.e. assuming the field does not vary on the effective scales of the spacecraft motion). Moreover, this method assumes that all measurement points are situated inside or surround the same current sheet.

This technique has been recently applied by Vallat et al. (2005), using Cluster 4-point magnetic field data to partially survey the ring current in the evening and post-midnight sectors. Their study was limited by the data taken during 2002, but suggested that the ring current can extend from -65 to 65° in latitude all over the evening and post-midnight sectors about 9 h of MLT. The present paper extends the study of Vallat et al. (2005) to survey the distributions of the ring current at all MLT and discuss the locations of the connecting region 2 field-aligned currents (FACs).

2 Results

2.1 Observations from single pass

Figure 1 shows an example orbit of the Cluster spacecraft S/C1 between 05:00 and 18:00 UT on 6 February 2004. The plot shows the X-Z plane, in SM coordinates, and the configuration of all 4S/C (expanded by a factor of 80) at intervals along the track every 2 h. Geomagnetic field lines are drawn using the T96 model (Tsyganenko and Stern, 1996), for the average prevailing conditions: solar wind dynamic pressure, $P_{\rm dyn} = 1.76$ nPa, IMF $B_{\rm Y} = -3.89$ nT, IMF $B_{\rm Z} = -2.29$ nT, and Dst $= -18$ nT. The spacecraft moved from the pre-midnight sector (21:00 MLT) and south of the magnetic equator through perigee at 11:31 UT (1.6 MLT) to the pre-midnight sector (13.8 MLT) and north of the equator. The spacecraft passed through or near the ring current near to perigee. The average separation between the four Cluster spacecraft was about 480 km and the configuration was a nearly regular tetrahedron.

Figure 2 shows an overview of the results from the curlometer technique (Dunlop et al., 2002) during this pass (09:31 to 11:31 UT). Figure 2 shows (a) the magnetic field magnitude, (b) the $J_{\rm X}$, $J_{\rm Y}$, $J_{\rm Z}$ and J_ϕ components of current density in cartesian and polar SM coordinates, (c) the ratio Div($\boldsymbol{B}$)/|Curl($\boldsymbol{B}$)|, and (d) the total current density; the horizontal axis is labelled by the MLT, latitude (LAT) and radial distance (R) of the spacecraft locations in SM coordinates, as well as the hours around perigee and UT. The approximate times of entry into and exit from the ring current region of Cluster 1 are highlighted by the grey region between the two red vertical dashed lines. These boundaries were determined by significant increase in the proton flux at higher energies (above ~95 keV) observed by RAPID (Wilken et al., 2001) and by sharp decrease observed simultaneously by CODIF (Rème et al., 2001) at lower energy ranges (up to 40 keV) (data not shown). From Fig. 2, we find the 4 spacecraft observed almost the same magnetic field structures and that the results are stable within the marked region of the ring current encounter. The results using the curlometer technique are therefore reliable. From Fig. 2b, however, we find the three components of the current were highly variable during this pass before entry into and after exit from the ring current region, which Woodfield et al. (2007) and Zhang et al. (2010) explain in terms of the effect of the region-2 FACs. In the ring current, the current was stable, and $J_{\rm Z}$ components in SM coordinates were near zero, $J_{\rm Y}$ was mainly positive (duskward) with an average value of about 15 nA m^{-2}, and $J_{\rm X}$ was mainly negative (tailward) with an average value of about 10 nA m^{-2}, while J_ϕ was mainly negative (tailward)

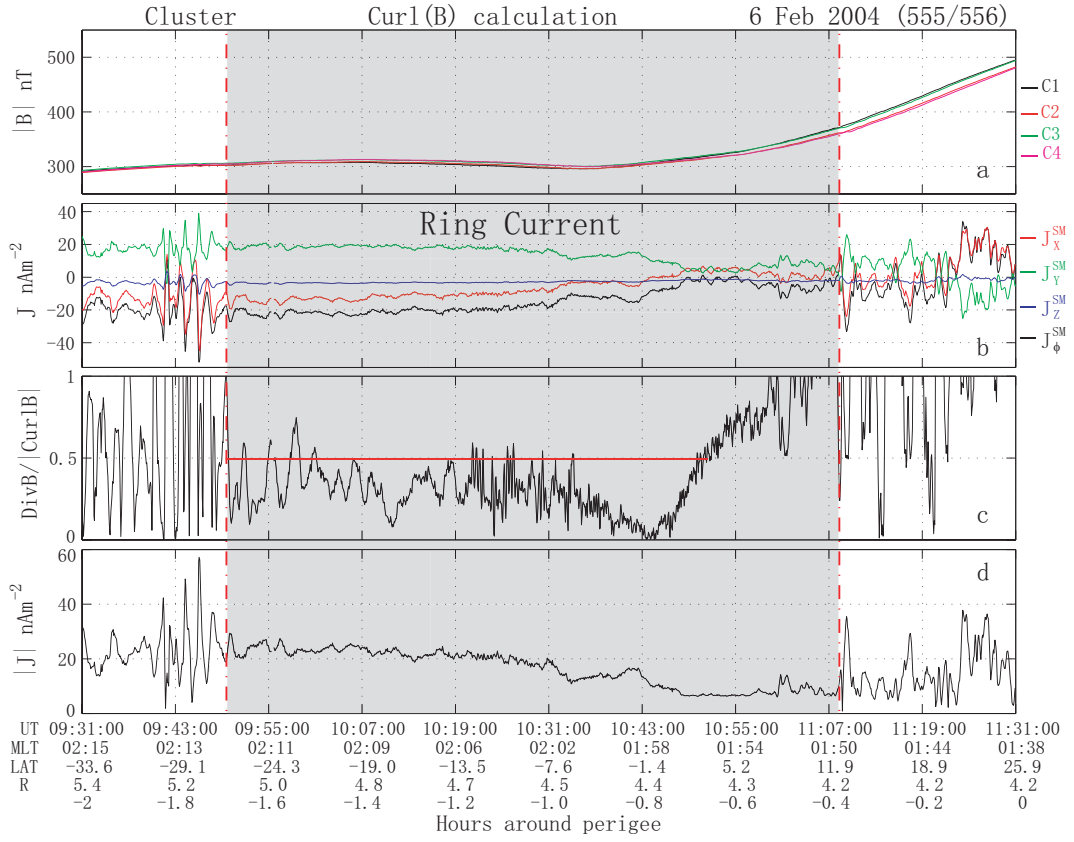

Fig. 2. An overview of the results calculated from 4 Cluster spacecraft technique (Curlometer) during 09:31 to 11:31 UT on 6 February 2004: **(a)** the magnitude of magnetic field observed by 4 Cluster spacecraft, **(b)** the J_X, J_Y, J_Z and J_ϕ components of current density in cartestian and polar SM coordinates, **(c)** Div(B)/|Curl(B)|, and **(d)** the total current density.

with an average value of about 20 nA m^{-2} (see Fig. 2b). These components show that the ring current lies mainly in the equatorial SM plane, directed duskward and tailward at 1.6 MLT. In Fig. 2c, the Div($\boldsymbol{B}$)/|Curl($\boldsymbol{B}$)| ratio is seen to have been highly variable and often >1 before entry into and after exit from the ring current region. Nevertheless, it was stable and mainly <0.5 (under red line) within the interval of the ring current. Dunlop et al. (1988) suggested that the ratio Div($\boldsymbol{B}$)/|Curl($\boldsymbol{B}$)| can provide a quality estimate for $\boldsymbol{J}_{\text{calculated}}$ in place of the unknown error ($\boldsymbol{J}_{\text{calculated}} - \boldsymbol{J}_{\text{real}}$) when the shape and orientation of the spacecraft configuration is regular tetrahedron, and the magnetic field structure is nearly isotropic within the tetrahedron. The use of Div($\boldsymbol{B}$) does not give a direct indication of the actual error in the current estimate and is less relevant for distorted tetrahedral configurations. Because a very long or a very flat tetrahedron (the elongation (E) or planarity (P) of the tetrahedron is greater than 0.9) will lead to an estimated error reaching 10 % and more, estimates of the absolute uncertainty in the calculation of curl B were also made (see discussion in Robert et al., 1998; Dunlop et al., 2002, and Vallat et al., 2005). These authors showed that the curlometer results are reliable when the Div($\boldsymbol{B}$)/|Curl($\boldsymbol{B}$)| < 0.5, depending on the temporal stability of the current. In fact, all values of the ring current above a few nA m^{-2} are, in principle, measurable by the curlometer and the use of Div($\boldsymbol{B}$)/|Curl($\boldsymbol{B}$)| is as a threshold indicator only. We use this as a criterion to select reliable results from all the passes in the year studied. The stability of the calculation can be independently tested by rotating the spacecraft order in the curlometer calculation, and we estimate the maximum error in $|\boldsymbol{J}|$ is below 20 % for the selected cases. The deduced $|\boldsymbol{J}|$, ranged from 10 to 27 nA m^{-2} within the ring current, which is well above the measurable limit of the technique and in fact the results here depend only on J_ϕ, which is the most accurate component of J.

2.2 Observations from one year of passes

Figure 3 shows the plots of the ϕ components of the current density in SM coordinates near Cluster perigee crossings between 14 July 2003 (195/2003) and 27 April 2004 (118/2004). Each vertical strip is a section of an orbit – the x-axis is the orbit number, y-axis is time relative to perigee, and the colour scale is the value of (a) $\boldsymbol{J}^{\text{SM}}_\phi$ and (b) Div($\boldsymbol{B}$)/|Curl($\boldsymbol{B}$)|. From Fig. 3b, we find that the ratio of Div($\boldsymbol{B}$)/|Curl($\boldsymbol{B}$)| was near or over 1 for most of the

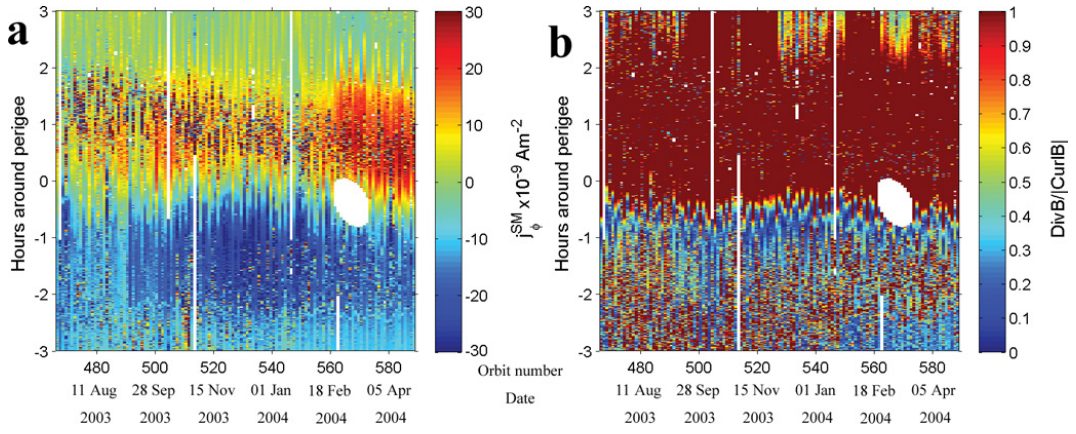

Fig. 3. Plots of ϕ components of the current density in SM coordinates around Cluster perigee crossings between 14 July 2003 (195/2003, orbit number 468) and 27 April 2004 (118/2004, orbit number 589). Each vertical strip is a section of an orbit – the x-axis is the orbit number, y-axis is time relative to perigee, and the colour scale is the value of $\boldsymbol{J}_{\phi}^{\mathrm{SM}}$ and Div($\boldsymbol{B}$)/|Curl($\boldsymbol{B}$)|, for the panels of **(a)** and **(b)**, respectively.

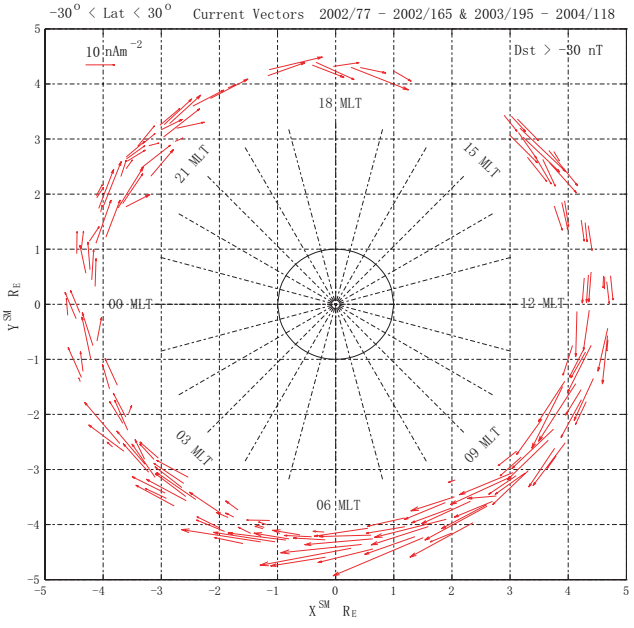

Fig. 4. The distributions of ring current around the equator plane in SM coordinates around Cluster perigee crossings between 18 March 2002 (77/2002, orbit number 265) and 14 June 2002 (165/2002, orbit number 302) and between 14 July 2003 (195/2003) and 27 April 2004 (118/2004). The vectors represent the directions and magnitude of the current density in XY plane.

time between about −0.5 h before to 3 h after a perigee crossing (period A), while the ratio was mainly less than 0.5 between −1.2 and −0.5 h relative to perigee (period B) and was mainly near 1 between −3 and −1.2 h relative to perigee (period C). This is because the spacecraft were crossing region 2 and region 1 FACs and/or the cusp FACs in periods A and C, but traversing the central ring current region in period B. This confirms that the curlometer results are generally reliable in the ring current region, where the $\boldsymbol{J}_{\phi}$ component was almost always negative. These values show the expected westward ring current around the equator. The morphology of the ring current system suggested by Iijima et al. (1990) and Le et al. (2004) partially closes in the ionosphere via up and down Region 2 FACs, and the ring current can extend from −65 to 65° in latitude all over the evening and post-midnight sectors (Vallat et al., 2005). Considering the effect of the FACs on the accuracy of the current calculations, we focus here on the results in the equatorial plane (−30 to 30°).

Using the criterion Div($\boldsymbol{B}$)/|Curl($\boldsymbol{B}$)| < 0.5 with a regular tetrahedron configuration, we selected all reliable results in the ring current when the Dst index is greater than −30 nT (more positive than −30 nT, i.e. non-storm conditions) and averaged them over 5-min intervals. The current vectors, shown in Fig. 4, are projected onto the XY plane in SM coordinates. The full azimuthal ring of current density observations at non-storm times has been obtained using almost a full year of data from 18 March 2002 to 14 June 2002 and from 14 July 2003 to 27 April 2004. Note, however, in Fig. 4 that there are a few white gaps due to missing data or lack of reliable data. In addition, the vectors are averaged over intervals of stable current vectors, which typically do not vary during each pass and therefore are only slightly dependent on the actual number of data points available. In fact, the fluctuation in current through the region during each pass is not significant compared to the general error in Curl($\boldsymbol{B}$). The basic error in Curl($\boldsymbol{B}$) is around 5–20 %, which is larger than the typical fluctuation in ring current values as most intervals within the ring current do not show large variations. Thus, the error arising from selection of a larger or smaller data interval is very small compared to the other uncertainties of measurement. In addition, we should note that the distribution of current vectors, in azimuth, is only a result of the Cluster spacecraft orbital constraints.

3 Discussion

Figure 4 shows the nearly full-circle distribution of the ring current for non-storm periods. The distribution is asymmetric, where the magnitudes are markedly enhanced between about 05:00 and 11:00 MLT and are reduced between about 12:00 and 17:00 MLT (between 17:00–24:00 MLT they are only slightly enhanced and appear to reduce again after 24:00 MLT along the nightside ring). This behaviour is notable since it is opposite to that reported by Jorgensen et al. (2004), for example, where the peak of the ring current occurs in the afternoon sector for quiet conditions. The current vectors between 05:00 and 11:00 MLT found here are, on average, a factor of 2 greater than in other sectors – a rather large asymmetry. We therefore investigate further what factors might drive the asymmetric distribution. These questions will be studied further in a later paper, but we attempt to show the plausible effects below.

Firstly, there may be a dependence on geomagnetic activity, which would also arise as a seasonal effect because the Cluster orbit samples MLT at different times of the year. Secondly, we note that Cluster samples the ring plane only in the radial range ∼4–4.5 R_E, so that any adjustment of the radial profile of current density (which varies with MLT) is not well sampled. It is certainly possible that the higher current density seen here could result from a narrower density profile in that range of MLT. Other adjustments of the ring plane distribution could replicate these results without changing the overall, westward current in the ring. This scenario, however, does not itself suggest a source for the asymmetry. Thirdly, we can state that the asymmetry is at least consistent with a re-configuration of the whole current system into the polar ionosphere through connection to the region 2 FACs and ionospheric currents. Thus, the downward FACs (centered on 14:00 MLT) will naturally extract current (potentially) from the duskside ring plane, while the upward FACs (centered on 09:00 MLT) will deposit current into the dawnside ring plane.

In order to make a more quantitative investigation, we averaged the current density $|J|$ and the corresponding Dst and AE indexes in every MLT one hour bin (or 15° in XY plane) and we show comparisons of these parameters in Fig. 5. Figure 5a, b, and c shows the MLT distributions of the one hour average current density $|J|$ (from Fig. 4) and the corresponding MLT distributions of the Dst and AE indices, respectively. Figure 5d, e, and f shows scatter plots of the average current density $|J|$ against the Dst and AE indices, and AE against Dst, respectively. The red lines present linear fitted lines of the scatter points, but are primarily shown here to guide the eye, since the trends are not simply linear.

From Fig. 5a, we can confirm that the average magnitudes of the measured current density at the Cluster ring plane crossing (∼4–4.5 R_E) ranged from 9 to 27 nA m^{-2}, which are greater than the quiet time averages of ∼1–4 nA m^{-2} derived using the Parker equation from observed magnetic field and particle pressures (but then estimated over the range of L-values 2–9; see Lui and Hamilton, 1992, and De Michelis et al., 1999). This difference has been accounted for by Vallat et al. (2005) who also used the Curlometer technique, deriving similar values of 30 nA m^{-2} to our study. The profile of $|J|$ also confirms that there is an enhancement in the morning sector and a dip in after noon. In fact, the trends shown there could be viewed as a steady growth of current density (from 10–27 nA m^{-2}) in the MLT range from about 12:00–02:00 UT, and a less steady depletion of current density (from 20–10 nA m^{-2}) in the MLT range from about 24:00–12:00 UT. The growth in current appears to increase at around 09:00 MLT and dips further at around 16:00 MLT. Furthermore, the dip in value between 00:00 and 02:00 MLT is also apparent. Although further work is needed to fully assess the effect of: (1) observation limitations in the observations (such as spatial gradient errors in the use of time series data); (2) the dependence of the current density values on Dst (generally regarded as a poor parameter), together with our use of non-storm (Dst > -30 nT) as opposed to quiet activity levels, and (3) the quality requirement Div($\boldsymbol{B}$)/|Curl($\boldsymbol{B}$)| $<$ 0.5 which may reduce the averages slightly by removing the lowest J-values, we nevertheless feel a number of suggestions arise from the MLT trends revealed here.

For example, Fig. 5b and c, showing the average geomagnetic activities, confirm that the periods we investigated are under relatively quiet or non-storm conditions, although AE shows clearly enhanced activity between about 03:00 and 15:00 MLT and may account for part of the increased range of $|J|$ values for those MLT values. This change in AE level however is a relatively small effect (changing from an average of about 200 nT to about 150 nT for other MLT), and we note that the variability seen in both AE and Dst from MLT bin to bin is large compared to the difference in mean values. Such variability is not reflected in the Cluster in situ sampling of $|J|$ and therefore the current density does not respond significantly to changing activity. The trends in AE, furthermore, show a distinctly opposing effect to that seen in $|J|$: in the range 02:00–14:00 MLT, the running average of AE is slowly decreasing from 12:00 to 02:00 MLT while the current grows. Before 12:00 MLT, the correlation is less clear since AE shows little obvious trend here. Nevertheless, it is worth pointing out that the values in the MLT bins correspond to times of the year when Cluster samples that bin, hence the effect is also seasonal. The parameter Dst represents, in some sense, the overall current in the ring, although it is recognized that it is a rather poor parameter and contains effects from the time history of activity prior to its determination. The variability from bin to bin is large but the underlying trend does follow that of $|J|$ from 12:00 to 06:00 MLT. The profile of Dst seen between 12:00 and 24:00 MLT is broken at about 18:00 MLT, however, and between 00:00 and 06:00 MLT the correlation is also poor.

Figure 5d, e, and f shows the correlations in more detail. These scatter plots indicate that the magnitudes of the current

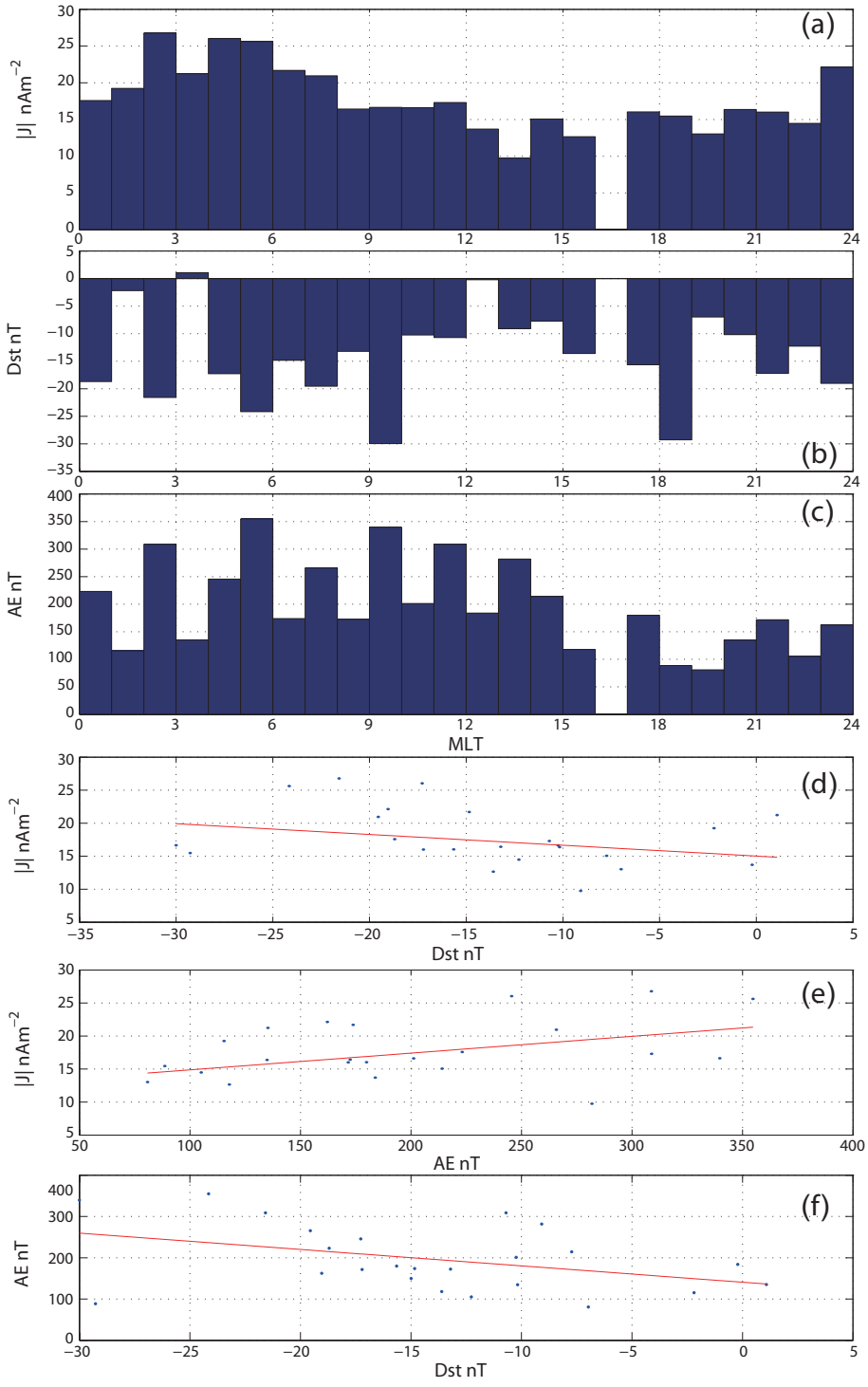

Fig. 5. The MLT distributions of the one hour average current density $|J|$ (from Fig. 4) and the corresponding MLT distributions of the Dst and AE indices, respectively, together with the scatter plots of this average current density $|J|$ against Dst and AE indices, and AE against Dst, respectively.

density are fairly independent of the geomagnetic activities, although there is a slight trend as indicated by the red lines: the plot of $|J|$ against AE shows that a higher geomagnetic activity corresponds to a lager current density, for example, although the scatter increases with increasing AE. The plot of $|J|$ against Dst shows that the correlation, if present, is

not linear: the value of $|J|$ does fall with Dst in the range -20 to -10 nT, but increases in the range -30 to -20 nT and increases again between -10 to 0 nT. For the plot of AE against Dst, we see that although there is a good correlation between -25 and -12 nT (in Dst), there is no clear trend between -12 and 0 nT. This shows that the values obtained for Dst do not always follow those for AE.

We therefore suggest that the trends seen in AE and Dst cannot fully account for the trends seen in the current density. As mentioned, it is possible that the asymmetry in $|J|$ simply reflects an ordered change in the radial profile of the current density, so that the reduction in the local $|J|$ at Cluster does not reflect a reduction in the total westward current flowing in the ring. However, we do not have an obvious mechanism to drive this change in mind, and in fact the enhanced current vectors are measured over the widest radial range for that range of MLT and suggest a well-defined, broad peak in $|J|$. Alternatively, we propose that the asymmetry is also consistent with the linkage to region 2 FACs, which map down to the ionospheric currents. For example, the growth of the current as it flows westward across the morning sector could indicate that the region 2 FACs, which are upward from the ionosphere, feed into the ring current around 09:00 MLT, and the decay as the current flows across the afternoon sector could reveal a downward FAC current around 14:00 MLT. These region 2 currents connect to Pedersen currents across the auroral oval (equatorward before noon and poleward afternoon) and are related to sunward Hall currents along the auroral oval (Untiedt and Baumjohann, 1993). Thus, the region 2 currents associated with the longitudinal gradients in the ring current are related to the auroral electrojets. The use of low Dst disturbance levels means that relatively non-storm times have been studied here, so that the DP-2 current system will dominate. For the growth phase currents the region 2 FACs will be relatively close to noon (Cowley and Lockwood, 1992), consistent with the ring current decrease in Fig. 4 being localized relatively near noon. The question of how the whole current system resulting from the asymmetric ring current is configured in the polar ionosphere, and in particular the connection of the region 2 FACs with ionospheric currents, will be studied in a later paper.

4 Conclusions

We have investigated an almost full year of magnetic field data from the four Cluster spacecraft at times when they had small separations, nearly regular tetrahedral configurations, and Dst was greater than -30 nT (non-storm times). By using the multi-spacecraft curlometer technique, we have directly calculated the current distributions near the Cluster perigee crossings, confirming they have sufficient accuracy to obtain full-circle (all magnetic local times), unambiguous estimates of in situ ring current densities for the first time. The data are taken during non-storm periods, where all samples reveal a westward current near the equator and indicate that this quiet time average westward ring current flow is asymmetric in magnetic local time (MLT) and has an average current density between 9 and 27 nA m^{-2}.

The direction of current is shown to be very well ordered for the whole range of MLT, in line with previous studies on partial ring extent (Vallat et al., 2005). The magnitude of the current density is sampled in the radial range accessed by Cluster ($\sim$4–4.5 R_E), where the distinct asymmetry revealed grows from 10 to 27 nA m^{-2} as azimuth reduces from about 12:00 MLT to 03:00 MLT; and falls from 20 to 10 nA m^{-2} (less steadily than the growth) as azimuth reduces from 24:00 to 12:00 MLT. This result has not been reported before and we suggest it could reflect a number of effects.

Firstly, we argue it is at least consistent with the operation of region-2 field aligned-currents (FACs), which flow upward into the ring current around 09:00 MLT and downward out of the ring current around 14:00 MLT. This scenario, although unconfirmed and requires further study, does provide a possible mechanism driving the asymmetry, so that region 2 FACs connecting from the ring current into the auroral and ionospheric region help configure the current system in the polar ionosphere. In its favour, connectivity to the region 2 FAC system is one of the few mechanisms which can apparently achieve the particular asymmetry observed (particle injection and drift effects having the opposite contribution to the expected current). The scenario, however, assumes that the current density measured at the local crossings of Cluster does not substantially redistribute within the ring, as could be the case.

We therefore note that the effect is also consistent with an MLT asymmetry in the radial distribution profile of current density (which results in higher or lower peak values in MLT, centered on radial distances at $\sim$4–4.5 R_E), while maintaining the total flow of westward current. This second scenario, therefore, does not require connection via the FAC system. Nevertheless, it should be noted that inspection of Fig. 4 shows that the observed current densities which are enhanced are actually sampled from the widest radial range so that the peak in $|J|$ in this range of MLT is actually broad and well defined. Moreover, this option does not provide an assumed mechanism to drive such a redistribution of current. Finally, it was noted in the Discussion (Sect. 3) that part, but not all, of the current density enhancement could reflect an observed increase in the mean AE activity during the times when Cluster sampled those MLT, so that the effect is perhaps made more significant by changes in activity.

Acknowledgements. This work is supported by the Natural Science Foundation of Shanghai, China (grant No. 11ZR1441200), the National Natural Science Foundation of China (NSFC grant No. 41104091, 40890164, 41031064, 40874082) and Ocean Public Welfare Scientific Research Project, State Oceanic Administration People's Republic of China (No. 201005017). M. Dunlop is partly supported by Chinese Academy of Sciences (CAS) visiting Professorship for senior international scientists (Grant No. 2009S1-

54). The authors wish to express their gratitude to the UK research council NERC for funding this work through the GEOSPACE consortium, grant number NER/0/S/2003/00675. We thank the FGM Operations Team and FGM PI, E. A. Lucek for the data used.

Topical Editor R. Nakamura thanks three anonymous referees for their help in evaluating this paper.

References

Balogh, A., Carr, C. M., Acuña, M. H., Dunlop, M. W., Beek, T. J., Brown, P., Fornacon, K.-H., Georgescu, E., Glassmeier, K.-H., Harris, J., Musmann, G., Oddy, T., and Schwingenschuh, K.: The Cluster Magnetic Field Investigation: overview of in-flight performance and initial results, Ann. Geophys., 19, 1207–1217, doi:10.5194/angeo-19-1207-2001, 2001.

Cowley, S. W. H. and Lockwood, M.: Excitation and decay of solar-wind driven flows in the magnetosphere-ionosphere system, Ann. Geophys., 10, 103–115, 1992, http://www.ann-geophys.net/10/103/1992/.

Daglis, I. A., Thorne, R. M., Baumjohann, W., and Orsini, S.: The terrestrial ring current: Origin, formation, and decay, Rev. Geophys., 37, 407–438, 1999.

De Michelis, P., Daglis, I. A., and Consolini, G.: An average image of proton plasma pressure and of current systems in the equatorial plane derived from AMPTE/CCE-CHEM measurements, J. Geophys. Res., 104, 28615–28624, 1999.

Dunlop, M. W., Southwood, D. J., Glassmeier, K.-H., and Neubauer, F. M.: Analysis of multipoint magnetometer data, Adv. Space Res., 8, 273–277, 1988.

Dunlop, M. W., Balogh, A., Glassmeier, K.-H., and Robert, P.: Four-point Cluster application of magnetic field analysis tools: The Curlometer, J. Geophys. Res., 107, 1384–1387, 2002.

Escoubet, C. P., Fehringer, M., and Goldstein, M.: Introduction: The Cluster mission, Ann. Geophys., 19, 1197–1200, doi:10.5194/angeo-19-1197-2001, 2001.

Iijima, T., Potemra, T., and Zanetti, L.: Large]Scale Characteristics of Magnetospheric Equatorial Currents, J. Geophys. Res., 95, 991–999, 1990.

Jorgensen, A. M., Spence, H. E., Hughes, W. J., and Singer, H. J.: A statistical study of the global structure of the ring current, J. Geophys. Res., 109, A12204, doi:10.1029/2003JA010090, 2004.

Le, G., Russell, C. T., and Takahashi, K.: Morphology of the ring current derived from magnetic field observations, Ann. Geophys., 22, 1267–1295, doi:10.5194/angeo-22-1267-2004, 2004.

Lui, A. and Hamilton, D.: Radial Profiles of Quiet Time Magnetospheric Parameters, J. Geophys. Res., 97, 19325–19332, 1992.

Rème, H., Aoustin, C., Bosqued, J. M., Dandouras, I., Lavraud, B., Sauvaud, J. A., Barthe, A., Bouyssou, J., Camus, Th., Coeur-Joly, O., Cros, A., Cuvilo, J., Ducay, F., Garbarowitz, Y., Medale, J. L., Penou, E., Perrier, H., Romefort, D., Rouzaud, J., Vallat, C., Alcaydé, D., Jacquey, C., Mazelle, C., d'Uston, C., Möbius, E., Kistler, L. M., Crocker, K., Granoff, M., Mouikis, C., Popecki, M., Vosbury, M., Klecker, B., Hovestadt, D., Kucharek, H., Kuenneth, E., Paschmann, G., Scholer, M., Sckopke, N., Seidenschwang, E., Carlson, C. W., Curtis, D. W., Ingraham, C., Lin, R. P., McFadden, J. P., Parks, G. K., Phan, T., Formisano, V., Amata, E., Bavassano-Cattaneo, M. B., Baldetti, P., Bruno, R., Chionchio, G., Di Lellis, A., Marcucci, M. F., Pallocchia, G., Korth, A., Daly, P. W., Graeve, B., Rosenbauer, H., Vasyliunas, V., McCarthy, M., Wilber, M., Eliasson, L., Lundin, R., Olsen, S., Shelley, E. G., Fuselier, S., Ghielmetti, A. G., Lennartsson, W., Escoubet, C. P., Balsiger, H., Friedel, R., Cao, J.-B., Kovrazhkin, R. A., Papamastorakis, I., Pellat, R., Scudder, J., and Sonnerup, B.: First multispacecraft ion measurements in and near the Earth's magnetosphere with the identical Cluster ion spectrometry (CIS) experiment, Ann. Geophys., 19, 1303–1354, doi:10.5194/angeo-19-1303-2001, 2001.

Robert, P., Dunlop, M. W., Roux, A., and Chanteur, G.: Accuracy of current density determination, in Analysis Methods for Multispacecraft Data, ISSI Sci. Rep., SR-001, 395–418, 1998.

Singer, S. F.: A new model of magnetic storms and aurorae, Trans. AGU, 38, 175–190, 1957.

Tsyganenko, N. A. and Stern, D. P.: Modeling the global magnetic field of the large-scale Birkeland current systems, J. Geophys. Res., 101, 27187–27198, 1996.

Untiedt, J. and Baumjohann, W.: Studies of polar current systems using the IMS Scandinavian magnetometer array, Space Sci. Rev., 63, 245–390, 1993.

Vallat, C., Dandouras, I., Dunlop, M., Balogh, A., Lucek, E., Parks, G. K., Wilber, M., Roelof, E. C., Chanteur, G., and Rème, H.: First current density measurements in the ring current region using simultaneous multi-spacecraft CLUSTER-FGM data, Ann. Geophys., 23, 1849–1865, doi:10.5194/angeo-23-1849-2005, 2005.

Wilken, B., Daly, P. W., Mall, U., Aarsnes, K., Baker, D. N., Belian, R. D., Blake, J. B., Borg, H., Büchner, J., Carter, M., Fennell, J. F., Friedel, R., Fritz, T. A., Gliem, F., Grande, M., Kecskemety, K., Kettmann, G., Korth, A., Livi, S., McKenna-Lawlor, S., Mursula, K., Nikutowski, B., Perry, C. H., Pu, Z. Y., Roeder, J., Reeves, G. D., Sarris, E. T., Sandahl, I., Sraas, F., Woch, J., and Zong, Q.-G.: First results from the RAPID imaging energetic particle spectrometer on board Cluster, Ann. Geophys., 19, 1355–1366, doi:10.5194/angeo-19-1355-2001, 2001.

Woodfield, E. E., Dunlop, M. W., Holme, R., Davies, J. A., and Hapgood, M. A.: A comparison of Cluster magnetic data with the Tsyganenko 2001 model, J. Geophys. Res., 112, A06248, doi:10.1029/2006JA012217, 2007.

Zhang, Q.-H., Dunlop, M. W., Holme, R., and Woodfield, E. E.: Comparison of eight years magnetic field data from Cluster with Tsyganenko models in the inner magnetosphere, Ann. Geophys., 28, 309–326, doi:10.5194/angeo-28-309-2010, 2010.